

# GC–TOF-MS- and CE–TOF-MS-Based Metabolic Profiling of Cheonggukjang (Fast-Fermented Bean Paste) during Fermentation and Its Correlation with Metabolic Pathways

Jiyoung Kim,<sup>†</sup> Jung Nam Choi,<sup>†</sup> K. M. Maria John,<sup>†</sup> Miyako Kusano,<sup>‡</sup> Akira Oikawa,<sup>‡</sup> Kazuki Saito,<sup>‡</sup> and Choong Hwan Lee<sup>\*†</sup>

<sup>†</sup>Department of Bioscience and Biotechnology, Konkuk University, Seoul 143-701, Republic of Korea

<sup>‡</sup>RIKEN Plant Science Center, Yokohama 230-0045, Japan

**ABSTRACT:** Metabolic changes in fast-fermented bean paste (cheonggukjang) as a function of fermentation time were observed in inoculated *Bacillus* strains using gas chromatography time-of-flight mass spectrometry (GC–TOF-MS)- and capillary electrophoresis TOF-MS (CE–TOF-MS)-based metabolomics techniques. From the combined GC–MS and CE–MS analysis of fermented cheonggukjang samples, 123 metabolites were recovered (55% by GC–MS and 45% by CE–MS). Multivariate statistical analysis of fermented cheonggukjang samples showed that the separation of metabolites was influenced by the fermentation period (range, 0–72 h) and not by strain. When comparing the metabolites of fermented cheonggukjang with the metabolic pathways, uracil and thymine contents showed a rapid 20-fold increase after 24 h fermentation up to the end of fermentation. Xanthine and adenine levels increased slightly from 24 to 48 h fermentation and then decreased slightly at the end of fermentation. Hypoxanthine and guanine levels also increased remarkably during fermentation. Purine metabolism differed according to the microorganism used for cheonggukjang fermentation. Most intermediates in nucleoside biosynthesis were detected by CE–TOF-MS and were related to amino acid metabolism.

**KEYWORDS:** cheonggukjang, metabolite profiling, gas chromatography time-of-flight mass spectrometry (GC–TOF-MS), capillary electrophoresis time-of-flight mass spectrometry (CE–TOF-MS)

## ■ INTRODUCTION

Soybean and its fermented products are consumed as functional foods in many parts of the world. Cheonggukjang (CGJ) is a nutritious fermented traditional Korean food made from soybeans by using natural microflora such as *Bacillus* strains. It contains several vitamins, minerals, isoflavonoids, and soyasaponins as well as soy protein, fat, and carbohydrate metabolites; it is also known for its antioxidant, anti-inflammatory, antihypertensive, and antidiabetic activities.<sup>1,2</sup> These activities of CGJ are higher than those of raw soybean products.<sup>3</sup> Integrated tools are required to understand the complex processes that occur during fermentation and to define metabolic phenotypes. However, the relationship between metabolite changes and fermentation conditions has not yet been studied systematically.

Several studies have used the metabolomics approach to discover new and informative metabolites in biological systems.<sup>4,5</sup> Consequently, a range of analytical platforms, such as nuclear magnetic resonance (NMR), gas chromatography–mass spectrometry (GC–MS), capillary electrophoresis mass spectrometry (CE–MS), and liquid chromatography mass spectrometry (LC–MS), were developed.<sup>6</sup> These techniques were mainly used for metabolite phenotyping to identify and quantify the functional properties of samples.<sup>7</sup> GC–MS and CE–MS have been widely used in the fields of functional genomics and metabolomics to analyze whole organisms; they have also been extensively used to identify flavor compounds, volatile organic compounds, protein digests, and drug substances.<sup>8</sup> However, although there are several reports on

the relationships between metabolites and bioactivity in soybean and its fermented products,<sup>9,10</sup> no study has completely examined the changes in the CGJ metabolite profile as a function of fermentation time or has checked for correlations with metabolic pathways.

Here, we investigated the metabolic profile and metabolisms of CGJ during fermentation using GC–TOF-MS and CE–TOF-MS analyses. The metabolic pathway was related to both the abundance and the relative changes in the levels of metabolites with respect to fermentation times.

## ■ MATERIALS AND METHODS

**Chemicals.** All standards were purchased from Sigma. High-performance liquid chromatography (HPLC)-grade solvents were used for the analyses. [<sup>13</sup>C<sub>5</sub>]-Proline, [<sup>2</sup>H<sub>4</sub>]-succinic acid, [<sup>2</sup>H<sub>6</sub>]-2-hydroxybenzoic acid, [<sup>13</sup>C<sub>3</sub>]-myristic acid, [<sup>13</sup>C<sub>12</sub>]-sucrose, and [<sup>2</sup>H<sub>7</sub>]-cholesterol were purchased from Cambridge Isotope Laboratories (Andover, MA). <sup>13</sup>C<sub>5</sub>, <sup>15</sup>N glutamic acid, and [<sup>13</sup>C<sub>6</sub>]-glucose were purchased from Spectra Stable Isotopes (Columbia, MD). [<sup>2</sup>H<sub>4</sub>]-1,4-Diaminobutane was purchased from C/D/N ISOTOPES Inc. (Pointe-Claire, Quebec, Canada). [<sup>13</sup>C<sub>4</sub>]-Hexadecanoic acid was purchased from Icon (Mt. Marion, NY). The reagent for trimethylsilylation, *N*-methyl-*N*-trimethylsilyl trifluoroacetamide (MSTFA) with 1% trimethylchlorosilane (TMCS), was purchased from Pierce (Rockford, IL).

**Received:** July 2, 2012

**Revised:** August 17, 2012

**Accepted:** August 22, 2012

**Published:** August 22, 2012

**Preparation and Extraction of CGJ.** CGJ was provided by the Korea Food Research Institute (Sungnam, Korea). Ten kilograms of soybean (*Glycine max* L.) was inoculated (0.02%) with *Bacillus licheniformis* KCCM 11053P, 11054P, and *Bacillus amyloliquefaciens* CH86-1 in an incubator at 37 °C and fermented for 0, 12, 24, 36, 48, 60, and 72 h at 42 °C.<sup>4</sup>

For GC–MS analysis, each sample was extracted with 5 mg/mL water/methanol/chloroform (1:3:1 v/v/v) that included 10 stable isotope reference compounds (concentration, 15 ng/ $\mu$ L).<sup>11</sup> After centrifugation (5 min, 14 000g), the supernatant was transferred to a brown glass vial, and the extraction step was repeated twice. The extracts were dried before derivatization.<sup>12</sup> Methyl oxime derivatives were obtained by dissolving the dry extracts in 30  $\mu$ L of methoxyamine–HCl (20 mg/mL in pyridine) for 30 h at room temperature. After methoxylation, samples were trimethylsilylated for 1 h by adding 30  $\mu$ L of MSTFA with 1% TMCS at 37 °C with shaking. Next, 30  $\mu$ L of *n*-heptane was added after silylation. All derivatization steps were performed under a vacuum glovebox (VSC-1000; Sanplatec, Japan) filled with 99.9995% (G3 grade) dry nitrogen.

For CE–MS analysis, 5 mg of each CGJ material was extracted with 5 mg/mL methanol. The mixture was centrifuged at 5000 rpm for 10 min at 25 °C and then evaporated in vacuo. The resultant extract was filtered through a 0.22  $\mu$ m filter and used for metabolite profiling analysis.

**GC–TOF-MS Analysis.** For gas chromatography (GC)–TOF-MS analysis, each sample (1  $\mu$ L) was injected by a CTC CombiPAL autosampler (CTC Analytics, Zwingen, Switzerland) in splitless mode into an Agilent 6890N gas chromatograph equipped with a 30 m  $\times$  0.25 mm inner diameter (i.d.) fused-silica capillary column with a chemically bound 0.25  $\mu$ L film Rtx-5 Sil MS stationary phase (RESTEK, Bellefonte, U.S.) for metabolome analysis. Helium was used as the carrier gas at a constant flow rate of 1 mL/min. The temperature program for metabolome analysis started with a 2 min isothermal step at 80 °C, followed by temperature ramping at 30 °C to a final temperature of 320 °C, which was maintained for 3.5 min. Data acquisition was performed on a Pegasus III TOF-MS at an acquisition rate of 30 spectra/s in the mass range of  $m/z$  = 60–800.

**CE–TOF-MS Analysis.** All capillary electrophoresis (CE)–TOF-MS experiments were performed using Agilent CE system (Agilent Technologies, Waldbronn, Germany), Agilent G3250AA LC/MSD TOF system (Agilent Technologies, Palo Alto, CA), Agilent 1100 series binary HPLC pump, G1603A Agilent CE-MS adapter, and G1607A Agilent CE-electrospray ionization (ESI)-MS sprayer kit. G2201AA Agilent ChemStation software for CE and Analyst QS software for TOF-MS were used. Separations were carried out using a fused-silica capillary (50 cm i.d.  $\times$  100 cm total length) filled with 1 M formic acid for cation analyses or 20 mM ammonium formate (pH 10.0) for anion analyses as the electrolyte. The sample solutions were injected at 50 mbar for 15 s (15 nL). The applied voltage was set at 30 kV, capillary temperature was maintained at 20 °C, and the sample tray was cooled below 4 °C. Methanol/water (1:1 v/v) containing 0.5 M reserpine was delivered as the sheath liquid at 10 L/min. ESI–TOF-MS was conducted in the positive-ion mode for cation analyses or negative-ion mode for anion analyses, and the capillary voltage was set at 4 kV. A flow rate of heated dry nitrogen gas (heater temperature, 300 °C) was maintained at 10 psig. In TOF-MS, the fragmentor, skimmer, and octapole radio frequency (Oct RFV) voltages were 110, 50, and 160 V for cation analyses and 120, 60, and 220 V for anion analyses, respectively.

**Spectral Data Processing.** Raw GC–TOF-MS, CE–TOF-MS, and UPLC-Q-TOF data sets were exported to the NetCDF file (\*.cdf) format using the Databridge application manager using Masslynx software (version 4.1, Waters Corp), which was used to preprocess all data, including smoothing, alignment, time-window setting, and H-MCR. The resolved MS spectra were matched against reference mass spectra using the National Institute of Standards and Technology (NIST) mass spectral search program from the NIST/EPA/NIH mass spectral library (version 2.0). Peaks were annotated on the basis of retention indices (RIs) and the reference mass spectra comparison to the Golm Metabolome Database (GMD).

**Multivariate Analysis.** The resultant data matrix containing sample names as observations and peak area information as variables was processed using SIMCA-P software 12.0 (Umetrics, Umeå, Sweden) for multivariate analysis. The data sets were autoscaled (i.e., unit variance scaling) and log-transformed with the mean centered in a column-wise fashion prior to principal components analysis (PCA) and partial least-squares-discriminate analysis (PLS-DA) modeling.

**Metabolic Pathway Mapping.** Identified metabolites were mapped onto a search against *G. max* (soybean) in the Kyoto Encyclopedia of Genes and Genomes (KEGG) pathway maps.<sup>13</sup>

## RESULTS AND DISCUSSION

**GC–MS- and CE–MS-Based Metabolite Profiling of CGJ during Fermentation.** GC–TOF-MS and CE–TOF-MS were conducted to identify changes in metabolites during the fermentation of CGJ. From the 217 variables detected in the GC–MS analysis, 87 peaks were annotated by peak annotation using metabolite libraries (i.e., NIST02 and an internal in-house library database of RIKEN). In addition, 49 and 38 peaks from the 7820 and 3057 detected variables in the cation and anion modes, respectively, were annotated by CE–MS analysis. These peaks were reobtained from peak picking so that the data obtained from the GC–MS and CE–MS results were combined into a list of nonredundant metabolites with a relative low peak area threshold level or wide variations among samples. Consequently, considerable overlapping of peaks was observed when comparing the GC–MS and CE–MS data from cation (24 peaks) and anion (14 peaks) modes (Figure 1).

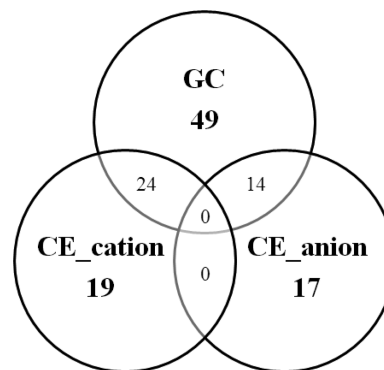


**Figure 1.** Venn diagram of the peaks obtained from gas chromatography–mass spectrometry (GC–MS) and capillary electrophoresis–mass spectrometry (CE–MS).

Finally, 123 annotated peaks were subjected to metabolite profiling and multivariate analysis. A complete list of all identified metabolites according to each analytical tool is provided in Table 1; the list contains about 40 amino acids (27 by GC–MS and 13 by CE–MS), 27 organic acids (19 by GC–MS and 8 by CE–MS), 19 carbohydrates (15 by GC–MS and 4 by CE–MS), 11 nucleosides (3 by GC–MS and 8 by CE–MS), 11 alcohols, 5 amines, 2 fatty acids (both by GC–MS), 7 various organic class compounds (4 by GC–MS and 3 by CE–MS), and 1 inorganic compound (by CE–MS).

PLS-DA is widely used for clustering nontargeted metabolic profiling data according to the vectors of numerous metabolites and comparing data obtained between various sample groups.<sup>12</sup> Figure 2A shows the PLS-DA scores with respect to CGJ fermentation time in the first two dimensions. According to the CGJ fermentation period, vectors  $t[1]$  and  $t[2]$  explained 41.0% and 12.5% of the variation between early fermentation (i.e., cooked soybean to 24 h fermented CGJ) and further

**Table 1. List of Metabolites from Cheonggukjang (CGJ) Fermentation Identified by Gas Chromatography– and Capillary Electrophoresis–Time-of-Flight–Mass Spectrometry (GC– and CE–TOF–MS)<sup>a</sup>**

no.	annotation	super class	no.	annotation	super class	no.	annotation	super class
1	alanine (2TMS)	amino acids	24	DL-glutamine (3TMS)	amino acids	47	DL-ornithine (4TMS)	amino acids
2	$\beta$ -alanine (3TMS)	amino acids	25	glutaric acid (2TMS)	organic acids	48	oxalic acid (2TMS)	organic acids
3	DL-asparagine (3TMS)	amino acids	26	2-hydroxy-glutaric acid (3TMS)	organic acids	49	3-methyl-2-[(trimethylsilyl)oxy]-pentanoic acid	organic acids
4	L-aspartic acid (3TMS)	amino acids	27	glycerol (3TMS)	alcohols	50	phenethylamine (2TMS)	amine
5	benzenepropanoic acid	organic acids	28	glycine	amino acids	51	DL-phenylalanine (2TMS)	amino acids
6	1,2,3,4-tetrakis[(trimethylsilyl)oxy]-butane	alcohols	29	glycolic acid (2TMS)	organic acids	52	phosphoric acid (3TMS)	inorganic
7	2,3-bis(trimethylsilyl)-butane	alcohols	30	hexadecanoate; palmitic acid	organic acids	53	phytol (1TMS)	alcohols
8	DL-2-aminobutyric acid (2TMS)	amino acids	31	L-histidine (3TMS)	amino acids	54	D-pinitol (5TMS)	carbohydrates
9	4-aminobutyric acid (3TMS); g-aminobutyric acid	amino acids	32	DL-homoserine (3TMS)	amino acids	55	3-amino-2-one-piperidin (2TMS)	organic
10	<i>trans</i> -caffeic acid (3TMS)	organic acids	33	hydroxylamine (3TMS)	alcohols	56	proline	amino acids
11	citric acid (4TMS)	organic acids	34	myo-inositol (6TMS)	carbohydrates	57	1,3-diamino-propane (4TMS)	amines
12	DL-cysteine (3TMS)	amino acids	35	DL-isocitric acid (4TMS)	organic acids	58	putrescine	amines
13	L-cystine (4TMS)	amino acids	36	isomaltose (1MEOX) (8TMS)	carbohydrates	59	pyroglutamate	amino acids
14	dihydrouracil (2TMS)	nucleosides	37	DL-lactic acid (2TMS)	organic acids	60	quinate	organic acids
15	D-fructose (1MEOX) (5TMS)	carbohydrates	38	D-lactose (1MEOX) (8TMS)	carbohydrates	61	R-(-)-1-amino-2-propanol (3TMS)	organic
16	fructose-6-phosphate (1MEOX) (6TMS)	carbohydrates	39	DL-leucine (2TMS)	amino acids	62	D-ribitol (5TMS)	alcohols
17	fumaric acid (2TMS)	organic acids	40	L-lysine (4TMS)	amino acids	63	D-ribose (1MEOX) (4TMS)	carbohydrates
18	galactinol (9TMS)	carbohydrates	41	DL-malic acid (3TMS)	organic acids	64	saccharic acid (6TMS)	organic acids
19	D-galacturonic acid (1MEOX) (5TMS)	organic acids	42	D-maltose (1MEOX) (8TMS)	carbohydrates	65	L-serine (3TMS)	amino acids
20	gluconic acid (6TMS)	organic acids	43	melibiose (8TMS)	carbohydrates	66	DL-N-acetyl-serine (2TMS)	amino acids
21	glucose	carbohydrates	44	DL-methionine (2TMS)	amino acids	67	shikimic acid (4TMS)	organic acids
22	glucose-6-phosphate (1MEOX) (6TMS)	carbohydrates	45	nicotinic acid (1TMS)	vitamin B3	68	<i>trans</i> -sinapic acid (2TMS)	organic acids
23	glutamate	amino acids	46	<i>n</i> -octadecanoic acid (1TMS)	organic acids	69	spermidine (5TMS)	amines
70	succinate	organic acids	89	2-hydroxyisobutyric acid	organic acids	108	anthranilic acid or trigonelline	amino acids or miscellaneous
71	sucrose	carbohydrates	90	allantoinate	organic	109	betaine	amino acids
72	DL-threonine (3TMS)	amino acids	91	calcium pantothenate	organic acid	110	choline+	amines
73	thymine (2TMS)	nucleosides	92	<i>cis</i> -aconitate	organic acids	111	citrulline	amino acids
74	$\delta$ -tocopherol (1TMS)	alcohols	93	citramalic acid	organic acids	112	cytidine	nucleosides
75	$\gamma$ -tocopherol (1TMS)	alcohols	94	D-galactosamine	carbohydrates	113	cytosine	nucleosides
76	$\alpha$ -trehalose (8TMS)	carbohydrates	95	glycerate	organic acids	114	D-glucosamine	carbohydrates
77	trimethylsilyl 3,5-bis(trimethylsilyl)-3-methylvalerate	organic acids	96	glycero-3-phosphate	miscellaneous	115	guanine	Nucleosides
78	tryptamine (3TMS)	amines	97	malonic acid	organic acids	116	guanosine	nucleosides
79	5-hydroxy-tryptamine (4TMS); serotonin	amines	98	mevalonolactone	lactone	117	homotyrosine	amino acids
80	DL-tryptophan (3TMS)	amino acids	99	N-acetyl-D-glucosamine	carbohydrates	118	homovaline	amino acids
81	tyramine (3TMS)	alcohols	100	N-acetyl-glutamic acid	amino acids	119	hydroxyproline	amino acids
82	L-tyrosine (3TMS)	amino acids	101	phenylpyruvate	organic acids	120	hypoxanthine	nucleosides
83	uracil (2TMS)	nucleosides	102	raffinose	carbohydrates	121	L-arginine	amino acids

Table 1. continued

no.	annotation	super class	no.	annotation	super class	no.	annotation	super class
84	urea (2TMS)	ketones	103	<i>trans</i> -aconitic acid	organic acids	122	L-isoleucine	amino acids
85	DL-valine (2TMS)	amino acids	104	xanthine	nucleosides	123	<i>N</i> - $\alpha$ -acetylmithine	amino acids
86	D-xylulose (1MEOX) (6TMS)	carbohydrates	105	adenine	nucleosides			
87	D-xylulose (1MEOX) (4TMS)	carbohydrates	106	adenosine	nucleosides			
88	2,6-diaminopimelate	amino acids	107	aminoadipate	amino acids			

<sup>a</sup>Nos. 1–87 detected by gas chromatography–mass spectrometry (GC–MS); nos. 88–104 detected by capillary electrophoresis mass spectrometry (CE–MS; anion); and nos. 105–123 detected by CE–MS (cation).

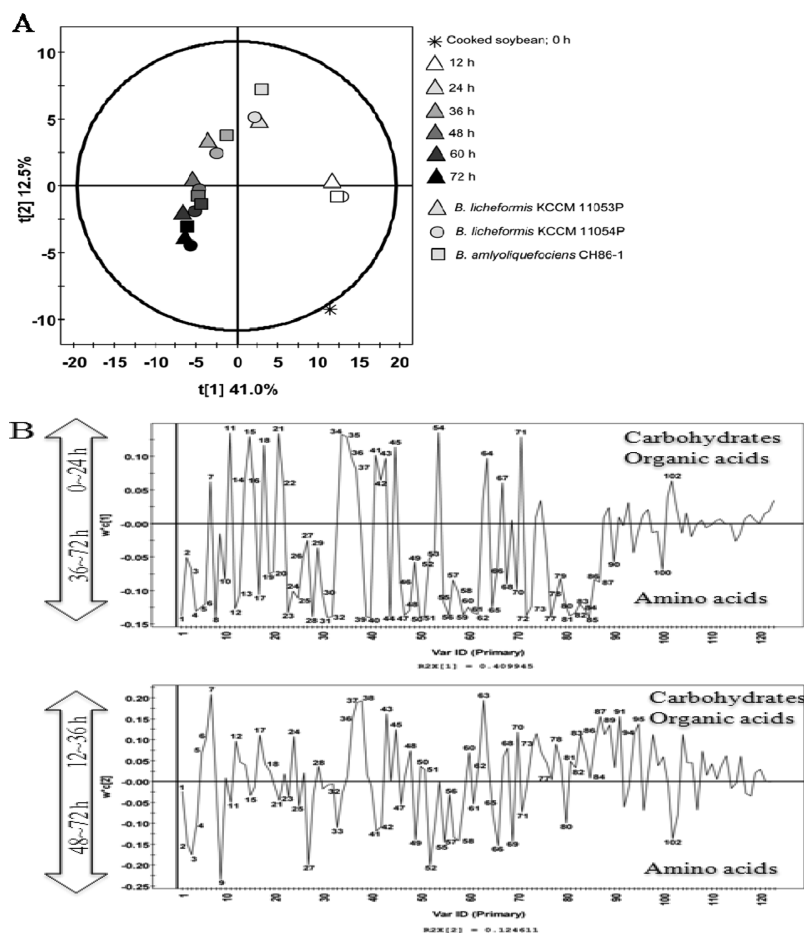


**Figure 2.** Partial least-squares-discriminate analysis (PLS-DA) of cheonggukjang (CGJ) fermentation. Score scatter (A) and loading (B) plots using  $t[1]$  and  $t[2]$  CGJ fermentation times.

fermentation (36–72 h). To determine significant differences in metabolites within these patterns, loading plots were used to compare the positive and negative axes at  $t[1]$  and  $t[2]$ , respectively (Figure 2B). In  $w^*c[1]$ , carbohydrates and organic acids were the major metabolites on the positive axis, contributing to early fermentation. Meanwhile, amino acids were the major metabolites on the negative axis, contributing to the later fermentation. The differentiation between the positive and negative axes at  $w^*c[2]$  was similar to that of metabolites classes to  $w^*c[1]$ . However,  $w^*c[2]$  contained unexplained metabolites at  $w^*c[1]$ .

**Metabolite Correlation of CGJ during Fermentation by GC–MS and CE–MS Analysis.** To compare the metabolite profiles under different fermentation conditions, pairwise correlational comparisons were conducted between all annotated 123 metabolites using a heat map (Figure 3). The metabolites on the heat map exhibited highly positive

correlational clustering as follows: amino acids and amino acids, organic acids, and various organic class molecules including amines and alcohols explained 21.4%, 20.6%, and 17.0% of the explained strong positive correlation, respectively ( $r > 0.85$ ; red color scheme). In contrast, the metabolites on the heat map showed highly negative correlational clustering as follows: amino acids and carbohydrates, amino acids and organic acids, and organic acids and carbohydrates explained 21.4%, 18.8%, and 13.8% of the strong negative correlation, respectively ( $r > -0.85$ ; blue color scheme). The number of rows above the heat map shows all annotated metabolites corresponding to Table 1. Each square indicates the Pearson correlation coefficient ( $r$ ) of a pair of 123 metabolites, and the values of  $r$  are represented by the intensity of blue (negative correlation) or red (positive correlation) as indicated on the color scale. The colors toward the right and bottom of the heat map are based on the metabolite class, where red represents

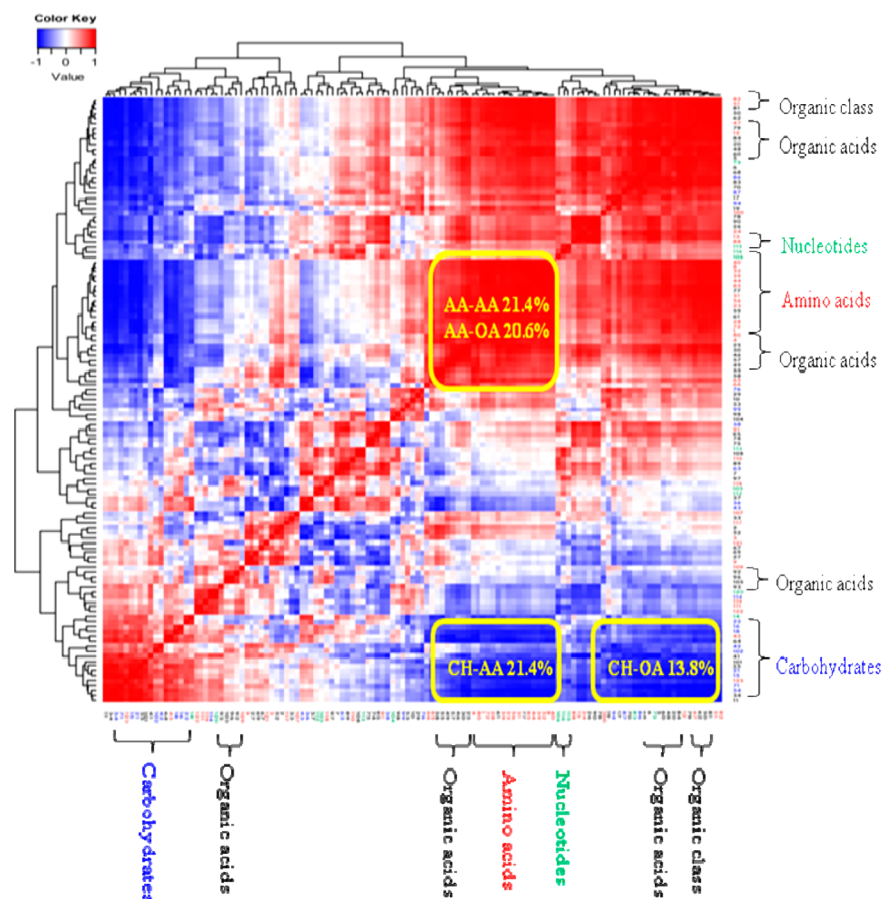


**Figure 3.** Heat map of metabolites according to detected metabolite peak areas from cheonggukjang (CGJ) fermentation.

amino acids; blue, carbohydrates; green, nucleosides; and black, organic acids and various organic super classes.

The use of combined systems for wider MS detection coverage has increased the number of metabolites that can be separated in a single analysis run.<sup>14</sup> About 123 annotated metabolites were identified by combining GC–MS and CE–MS, which is significantly more than the number of previously identified metabolites using only one analysis tool such as GC–MS (40 metabolites)<sup>4,15</sup> and LC–MS (37 metabolites).<sup>16</sup> About 55% and 45% of these metabolites were annotated by GC–MS and CE–MS, respectively. In general, dry soybean contains 40% protein, 35% carbohydrate, 20% lipid, and 5% ash contents (i.e., minerals).<sup>17</sup> After CGJ fermentation, these soybean components are converted into 32% amino acids, 22% organic acids, 15% carbohydrates, 9% nucleosides, 9% alcohols, and 13% various organic or inorganic classes. These results suggest that CGJ fermentation can significantly increase soybean protein digestibility by microbial enzymes, which leads to changes in the contents of fermented CGJ due to microorganism growth.<sup>18</sup> This shows that amino acids levels and composition increased and changed because of microbial metabolism during soy fermentation.

**Metabolic Pathway of Nucleotides during CGJ Fermentation.** The two types of nucleotide metabolism, pyrimidine (KEGG pathway map 00240) and purine (KEGG 00230) metabolism, were observed by CE–MS analysis during CGJ fermentation (Figure 4A). For pyrimidine metabolism, cytidine, cytosine, uracil, dihydrouracil, and thymine were detected, identified, and found to be related to  $\beta$ -alanine (KEGG 00410), arginine, and proline metabolism (KEGG

00330). Further, the nucleosides of the pyrimidine class were closely correlated. Among them, the uracil and thymine contents showed a rapid 20-fold increase after 24 h of fermentation up to the end of fermentation. The pyrimidine metabolism pattern was not significantly different between fermentation phases.

As shown in Figure 4B, the components identified for purine metabolism during CGJ fermentation included adenine, adenosine, hypoxanthine, xanthine, guanine, and guanosine and were correlated with histidine (KEGG 00340), glycine, serine, and threonine (KEGG 00260) metabolism. Xanthine and adenine levels increased slightly from 24 to 48 h fermentation and then decreased slightly at the end of fermentation. Hypoxanthine and guanine levels increased remarkably during fermentation and were related to histidine, glycine, serine, and threonine metabolism. Purine metabolism during CGJ fermentation differed depending on the microorganism used for fermentation. Guanosine, which is derived from guanine, increased rapidly in CGJ fermented with *B. amyloliquefaciens*, but decreased slightly in CGJ fermented with *B. licheniformis*. In addition, hypoxanthine levels showed a 10-fold increase after 24 h of fermentation when *B. amyloliquefaciens* was used; however, when *B. licheniformis* strains were used, the hypoxanthine levels showed a 10-fold increase only after 48–60 h of fermentation.

**Carbohydrates Metabolism during CGJ Fermentation.** The glycolysis (KEGG 00010) and citrate cycle (tricarboxylic acid [TCA] cycle; KEGG 00020) pathways in CGJ fermentation were correlated with the metabolism of certain amino acids such as tyrosine (KEGG 00350) and phenylalanine

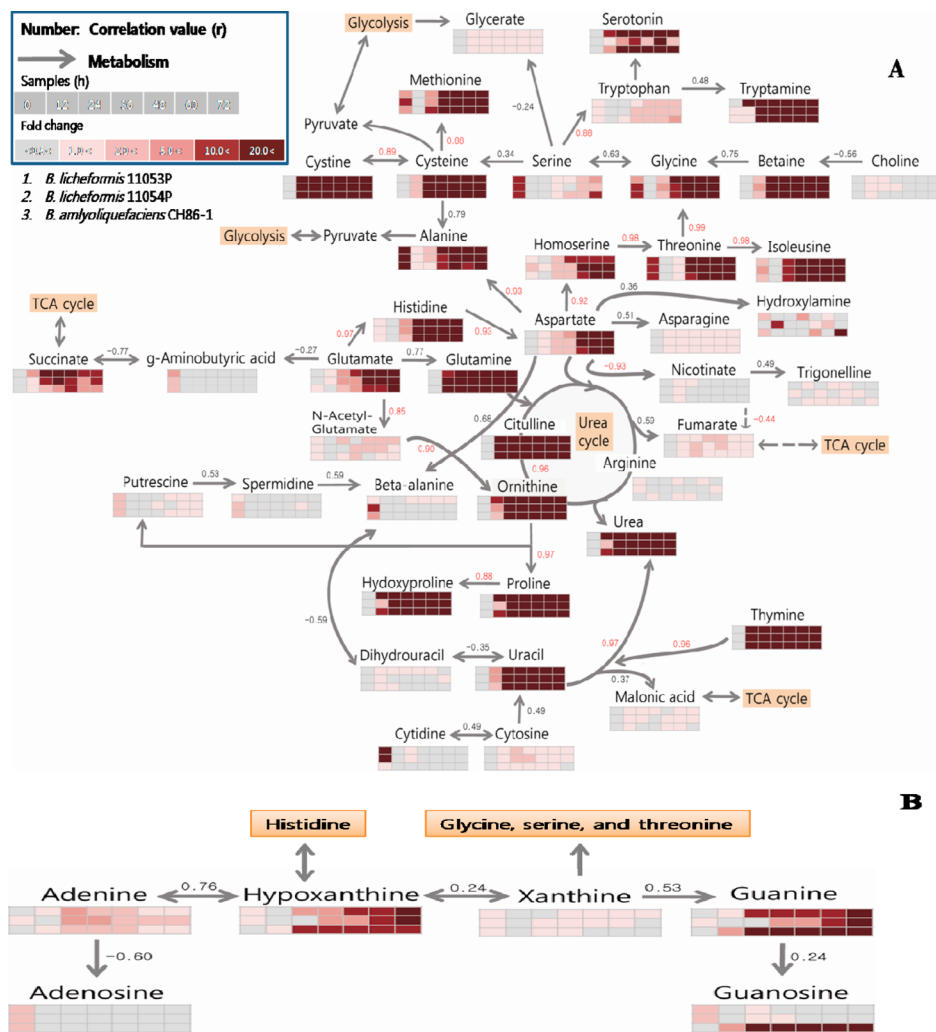


**Figure 4.** Schematic overview of changes in the metabolite pathway of cheonggukjang (CGJ) fermentation of three microorganisms. (A) Amino acid and nucleosides of pyrimidine metabolism; (B) nucleosides of purine metabolism.

(KEGG 00360) as well as secondary metabolism with the tocopherol (KEGG 00130) and mevalonate pathways (KEGG 00900) (Figure 5). During the CGJ fermentation process, trehalose, sucrose, glucose, and fructose levels decreased rapidly after 12 h fermentation. These changes in free sugar substrates, which upregulate glycolytic metabolism, subsequently altered the entire glycolysis pathway. As a result, glucose-6-phosphate, fructose-6-phosphate, and TCA cycle intermediates (e.g., citrate, *cis*-aconitate, isocitrate, fumarate, and malate) decreased during fermentation. The concentrations of tyrosine and phenylalanine were related to phosphoenolpyruvic acid (PEP), which is involved in glycolysis, and increased after 12 h fermentation to levels more than that observed in cooked soybean. Meanwhile, the levels of shikimate, which is correlated with tyrosine biosynthesis, decreased rapidly after 12 h fermentation.

Most intermediates in nucleoside biosynthesis were related to amino acid metabolism and mainly detected by CE–TOF–MS. Nucleotides are nitrogen compounds involved in energy metabolism and enzymatic reactions.<sup>19</sup> For pyrimidine metabolism, thymine and uracil levels increased with increasing fermentation time. Thymine, a pyrimidine nucleobase, is derived from the methylation of uracil at the fifth carbon; uracil helps complete the synthesis of many enzymes necessary

for cell function and is ultimately converted into urea.<sup>13</sup> Regarding purine metabolism, high hypoxanthine and guanine levels were observed during fermentation, which occur when guanine and adenine are converted into xanthine and hypoxanthine, respectively. These compounds are necessary additives in certain cell, bacteria, and parasite cultures as a substrate and nitrogen source.<sup>13</sup> Glycolysis and the levels of TCA cycle intermediates decreased because soluble sugars (i.e., glucose, fructose, maltose, and sucrose, etc.) as carbon sources are hydrolyzed by amylase and protease produced from *Bacillus* strains to provide energy for the growth of microorganisms during fermentation.<sup>20</sup> Melibiose, a disaccharide consisting of 1 galactose and 1 glucose molecule, is produced and metabolized only by enteric and lactic acid bacteria and other microbes; therefore, melibiose levels may increase and subsequently decrease slightly during fermentation.

The metabolite changes observed in this study during CGJ fermentation may enhance the functional properties of unfermented soybeans. Therefore, the results suggest that metabolomics approaches combining MS technologies provide a more comprehensive understanding of the metabolism involved in the production of fermented foods. Improved strategies can be obtained by combining analytical methods for identifying a wide spectrum of important metabolites associated

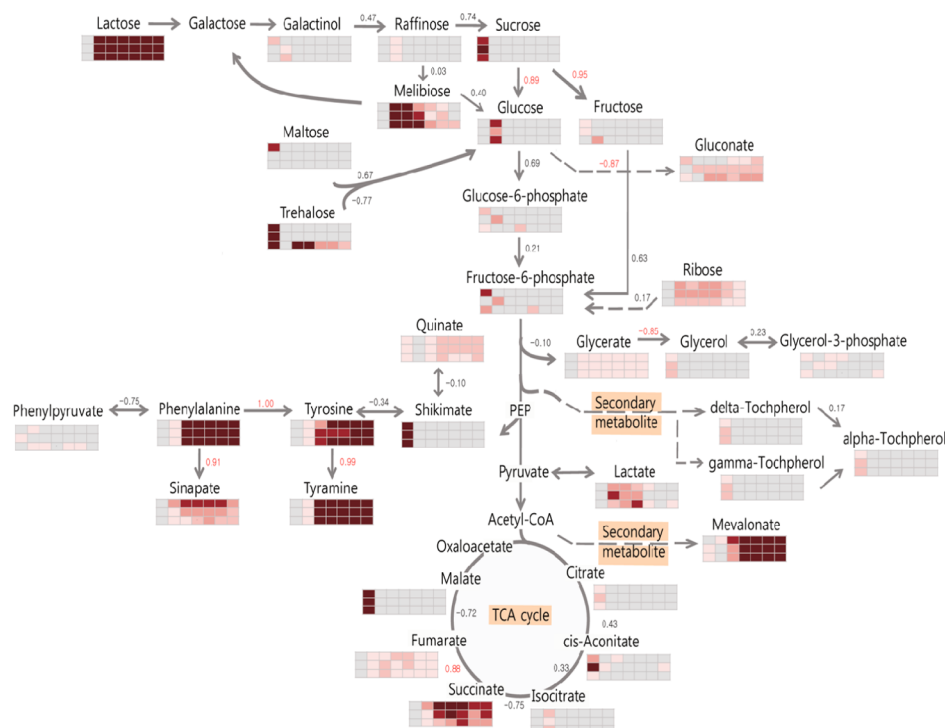


**Figure 5.** Schematic overview of changes in the metabolite pathway of cheonggukjang (CG) fermentation with that by carbohydrate metabolism of three microorganisms.

with physiological variations and understanding real-time information of fermentation.

## AUTHOR INFORMATION

### Corresponding Author

\*Tel.: +82 2 2049 6177. Fax: +82 2 455 4291. E-mail: chlee123@konkuk.ac.kr.

### Funding

This work was supported by the National Research Foundation of Korea (NRF) grant (MEST 2010-0019306 and 2010-0027204) and a grant from the Korea Healthcare Technology R&D Project (Grant No.: A103017), Ministry of Health & Welfare.

### Notes

The authors declare no competing financial interest.

## ACKNOWLEDGMENTS

We thank Makoto Kobayashi and Shoko Shinoda for their technical assistance.

## REFERENCES

- (1) Kim, N. Y.; Song, E. J.; Kwon, D. Y.; Kim, H. P.; Heo, M. Y. Antioxidant and antigenotoxic activities of Korean fermented soybean. *Food Chem. Toxicol.* **2008**, *46*, 1184–1189.
- (2) Kwon, D. Y.; Daily, J. W. I.; Kim, H. J.; Park, S. Antidiabetic effects of fermented soybean products on type 2 diabetes. *Nutr. Res. (N.Y., NY, U.S.)* **2010**, *30*, 1–13.
- (3) Choi, U. K.; Kim, M. H.; Lee, N. H.; Jeong, Y. S.; Kwon, O. J.; Kim, Y. C.; Hwang, Y. H. The characteristics of Cheonggukjang, a fermented soybean product, by the degree of germination of raw soybeans. *Food Sci. Biotechnol.* **2007**, *16*, 734–739.
- (4) Baek, J. G.; Shim, S. M.; Kwon, D. Y.; Choi, H. K.; Lee, C. H.; Kim, Y. S. Metabolite profiling of Cheonggukjang, a fermented soybean paste, inoculated with various *Bacillus* strains during fermentation. *Biosci. Biotechnol. Biochem.* **2010**, *74*, 1860–1868.

- (5) Choi, H. K.; Yoon, J. H.; Kim, Y. S.; Kwon, D. Y. Metabolomic profiling of Cheonggukjang during fermentation by <sup>1</sup>H NMR spectrometry and principal components analysis. *Process Biochem.* **2007**, *42*, 263–266.

- (6) Dunn, W. B.; Ellis, D. I. Metabolomics: Current analytical platforms and methodologies. *Trends Anal. Chem.* **2005**, *24*, 285–294.

- (7) Romina, B.; Cristiano, P.; Roberto, P.; Annagrazia, D. C.; Eugenia, B.; Charlotte, M.; Judith, W.; Alessandro, F.; Christof, S.; Sean, C.; Johannes, R.; Derek, S.; Luigi, C. Metabolomics and food processing: From semolina to pasta. *J. Agric. Food Chem.* **2011**, *59*, 9366–9377.

- (8) Kopka, J. Current challenges and developments in GC-MS based metabolite profiling technology. *J. Biotechnol.* **2006**, *124*, 312–322.

- (9) Fan, J.; Zhang, Y.; Chang, X.; Saito, M.; Li, Z. Changes in the radical scavenging activity of bacterial-type douchi, a traditional fermented soybean product, during the primary fermentation process. *Biosci. Biotechnol. Biochem.* **2009**, *73*, 2749–2753.

- (10) Jiyoung, K.; Jung, N. C.; Daejung, K.; Gun, H. S.; Young, S. K.; Hyung, K. C.; Dae, Y. K.; Lee, C. H. Correlation between antioxidative activities and metabolite changes during Cheonggukjang fermentation. *Biosci. Biotechnol. Biochem.* **2011**, *75*, 732–739.

- (11) Jonsson, P.; Gullberg, J.; Nordstrom, A.; Kusano, M.; Kowalczyk, M.; Sjostrom, M.; Moritz, T. A strategy for identifying differences in large series of metabolomic samples analyzed by GC/MS. *Anal. Chem.* **2004**, *76*, 1738–1745.

- (12) Kusano, M.; Fukushima, A.; Kobayashi, M.; Hayashi, N.; Jonsson, P.; Moritz, T.; Ebana, K.; Saito, K. Application of a metabolomic method combining one-dimensional and two-dimensional gas chromatography-time-of-flight mass spectrometry to metabolic phenotyping of natural variants in rice. *J. Chromatogr., B* **2007**, *855*, 71–79.

- (13) Wishart, D. S.; Knox, C.; Guo, A. C.; Eisner, R.; Young, N.; Gautam, B.; Hau, D. D.; Psychogios, N.; Dong, E.; Bouatra, S.; Mandal, R.; Sinelnikov, I.; Xia, J.; Jia, L.; Cruz, J. A.; Lim, E.; Sobsey, C. A.; Shrivastava, S.; Huang, P.; Liu, P.; Fang, L.; Peng, J.; Fradette, R.; Cheng, D.; Tzur, D.; Clements, M.; Lewis, A.; De Souza, A.; Zuniga, A.; Dawe, M.; Xiong, Y.; Clive, D.; Greiner, R.; Nazyrova, A.; Shaykhtudinov, R.; Li, L.; Vogel, H. J.; Forsythe, I. HMDB: a

knowledgebase for the human metabolome. *Nucleic Acids Res.* **2009**, *37*, D603–D610.

(14) Pan, Z.; Raftery, D. Comparing and combining NMR spectroscopy and mass spectrometry in metabolomics. *Anal. Bioanal. Chem.* **2007**, *387*, 525–527.

(15) Park, M. K.; Cho, I. H.; Lee, S.; Choi, H. K.; Kwon, D. Y.; Kim, Y. S. Metabolite profiling of Cheonggukjang, a fermented soybean paste, during fermentation by gas chromatography-mass spectrometry and principal component analysis. *Food Chem.* **2010**, *122*, 1313–1319.

(16) Kang, H. J.; Yang, H. J.; Kim, M. J.; Han, E. S.; Kim, H. J.; Jwon, D. Y. Metabolomic analysis of meju during fermentation by ultra performance liquid chromatography-quadrupole-time of flight mass spectrometry (UPLC-Q-TOF MS). *Food Chem.* **2011**, *127*, 1056–1064.

(17) John, J. B. A.; Sanford, C. G. The soybean as a source of bioactive molecules. In *Essentials of Functional Foods*; Schmidl, M. K., Labuza, T. P., Eds.; Aspen Publication: MD, 2000; pp 239–266.

(18) Pandey, A. Solid-state fermentation. *Biochem. Eng. J.* **2003**, *13*, 81–84.

(19) Stasolla, C.; Katahira, R.; Thorpe, T. A.; Ashihara, H. Purine and pyrimidine nucleotide metabolism in higher plants. *J. Plant Physiol.* **2003**, *160*, 1271–1295.

(20) Kim, E. J.; Hong, J. Y.; Shin, S. R.; Heo, H. J.; Moon, Y.-S.; Park, S. H.; Kim, K. S.; Yoon, K. Y. Taste composition and biological activities of Cheonggukjang containing *Rubus coreanum*. *Food Sci. Biotechnol.* **2008**, *17*, 687–691.